Research Article | Vol. 27, No. 15 | 22 Jul 2019 | OPTICS EXPRESS 20107

Optics EXPRESS

Highly stretchable hybrid silica/polymer optical fiber sensors for large-strain and high-temperature application

LIU YI[1,2] AND YU CHANGYUAN[3,*]

[1]*Photonic Research Centre, Department of Electrical Engineering, The Hong Kong Polytechnic University, Hong Kong, China*
[2]*School of Mechanical and Electronic Engineering, Wuhan University of Technology, Wuhan, Hubei Province, China*
[3]*Photonic Research Centre, Department of Electronic and Information Engineering, The Hong Kong Polytechnic University, Hong Kong, China*
[*]*changyuan.yu@polyu.edu.hk*

Abstract: The large-range and high-sensitivity strain measurement in high-temperature ambiance is a great challenge in engineering applications. Because of the frangibility of the glass material, the traditional optical fiber strain sensors cannot endure a limit strain of 1%. To break through the limit, we propose a hybrid silica/polymer optical fiber sensor. It can endure extraordinarily large strain. The maximum strain of 35% is confirmed by experiments. To achieve high sensitivity and detect a small change in strain, a phase tracking method is used. The sensitivity of the sensor is 28 pm/με which is 28 times larger than that of the traditional FBG sensors. In addition, because of the excellent high-temperature endurance of polyimide (PI) and adhesive, the sensor can survive in the high temperature up to 220 °C. The proposed hybrid silica/polymer optical fiber sensor has potentials to monitor deformation in plastic products, structure health in composite materials, and even strain in biomaterials.

1. Introduction

The strain is an important parameter to evaluate the health of civil structures and engineering equipment. In the past few decades, many strain sensors were developed for different applications. As an emerging technology, optical fiber sensors have attracted increasing attention, because of their immunity to electromagnetic interference, simple structure and compact size [1–3]. The strain sensors based on optical fiber technology has been used widely to monitor the health of railways, bridges, airfoils and machine tools [4–7]. Though the optical fiber made of silicon dioxide with a melting point of approximately 1700 °C has excellent high-temperature endurance, its limited stretchability severely restricts the dynamic range of strain measurement. The typical tensile strain limit of a fiber Bragg grating (FBG) is less than 4000 με (~0.4%) [8]. To overcome this shortcoming, various strain transferring methods and coating techniques have recently been investigated. Huang et al. reported a long-period fiber grating (LPFG) optic sensor packaged with a hybrid mechanism of elastic attachment and gauge length change in a high-temperature environment. The maximum strain was as high as 15200 με (~1.5%) [9]. Zhang et al. proposed an FBG sensor packaged by polydimethylsiloxane (PDMS) to monitor 2% strain of carbon fiber composite material on solid rocket motor [10]. Because of the low Yong's modulus, the packaging material weakens the strain from the host material and protect the fiber from break. However, the method also reduces the sensitivity of the sensors. The emerging polymer optical fiber (POF) is a good choice for large strain measurement. Many POF strain sensors were proposed [11,12]. Liu et al. wrote a Bragg grating sensor in a single mode POF. Its sensitivity is 1.44 pm/με with a 36100 με (3.61%) axial strain limit. Huang et al. implemented a single-mode-multimode-single-mode interference POF sensor with a large dynamic range of 20000 με

#362768 https://doi.org/10.1364/OE.27.020107
Journal © 2019 Received 21 Mar 2019; revised 17 May 2019; accepted 17 May 2019; published 8 Jul 2019

Optics EXPRESS

(2%) and a sensitivity of −1.72 pm/με. The POF fiber can maintain high sensitivity and large dynamic range of strain. However, the operating temperature of POF is lower than 100 °C. In many high-temperature applications, measuring large strain is still a difficult problem.

Comparing to the other optical fiber sensors, the Fabry–Perot (F-P) cavity sensor is unique. They have a breakpoint in the fiber. The discontinuous point can be used to release the strain and protect the sensor. Huang et al. designed an F-P sensor with a three-layer glass tube structure [13]. Each layer could stretch independently. The structure made the sensors achieve a large dynamic range of up to 120000 με (~12%). The freely stretchable and rigid glass multilayer structure is good for those applications that the sensors are fixed on the surface of the host. However, it will be invalid in the embedded applications. The multilayer glasses will be fixed by the continuous phase matrix in the composite materials and lose their mobility. A hybrid silica/polymer structure is a good choice to enhance the dynamic range of strain. Huang et al. proposed an interference sensor with silica fiber and epoxy adhesive. The maximum strain of 56.22% was confirmed [14].

In this paper, we implement a hybrid silica/polymer optical fiber F-P sensor prototype. A section of continuous polyimide (PI) tube is used to replace the complicated three-layer discontinuous glass tube. The F-P cavity consisting of a pair of end faces of silica optical fiber can stretch freely in the PI tube. The PI tube can not only be embedded into the composite materials and sustain the large strain, but also resist the high temperature of up to 220 °C. The maximum extension length of the F-P cavity can achieve 3500 μm, because of the high stretchability of the PI tube with a maximum strain of 350000 με (35%). It shows that the sensor can satisfy the large-strain and high-temperature requirement.

2. Principle of sensors

Figure 1(a) shows the structure of a hybrid silica/polymer F-P optical fiber sensor. The F-P sensor consists of two silica up-taper fibers and a PI tube with a length of L mm. The up-taper fibers used in the experiment are fabricated by a laser fusion tapering technique (Fujikura FSM-100). The CO_2 laser is focused on a standard commercial fiber (Corning SMF-28) with a core diameter of 8.2 μm and a cladding diameter of 125 μm, while the fiber is compressed with programmed moving platforms. The process increases the diameter of the fiber forming an up-taper fiber and eventually it is cleaved with a fiber cleaver. As shown in Fig. 1(a), two up-taper fibers with flat end faces are inserted into the PI tube to form an F-P cavity sensor. The fibers are fixed with a little of high-temperature adhesive at two ends of the tube, separated by a distance L. Figure 1(b) shows the signal interrogation system and calibration system of the sensors. The interrogator has a bandwidth ranging from 1510 to 1590 nm and a resolution of 1 pm. The light from the interrogator travels through the sensor, a part of the light is reflected at both cleaved end faces of the F-P cavity, producing a backward traveling interference signal. The optical interference signal is acquired by the interrogator. The interrogator can record the shift of the peaks and valleys in the spectrum automatically. To characterize the performances of the sensors, three calibration systems are used. The temperature calibration system is an oven whose temperature can be controlled by a computer. The large-strain calibration system is a couple of three-degree-of-freedom precision stages. The sensor is fixed on the stages and elongated by a large distance. The system can generate a large and precise strain load on the sensor. The small strain calibration system consists of a beam of uniform strength and a loading bar (which is not shown in the schematic diagram). When the sensor is adhesive on the top of the beam, the system can calibrate the strain with a high resolution.

Optics EXPRESS

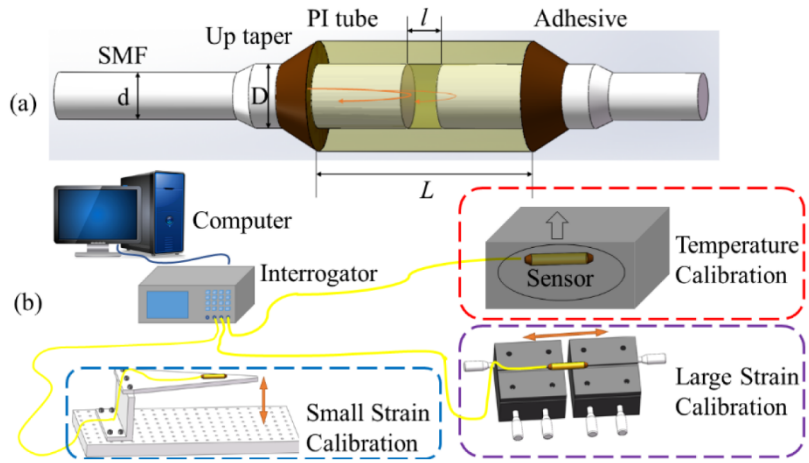

Fig. 1. (a) Schematic of a hybrid silica/polymer F-P optical fiber sensor structure and (b) the test system.

The tube used in our experiments is a commercial product whose hole is not an ideal circle. To assemble the F-P cavity in the tube, the fiber must be modified the diameter. The up-taper fibers are used. The microscope image of the up-taper fiber is shown in Fig. 2. To find the optimal diameter, many up-tapered samples are fabricated to match the hole of the PI tube. The optimal ratio of the diameters between the fiber and the hole is 153 μm: 160 μm. Because of the thick core of the up-taper, it becomes easy for the fiber to receive the reflected power from the second reflective mirror. The sensor has a higher anti-bending ability than those sensors fabricated by the standard single-mode fiber (SMF).

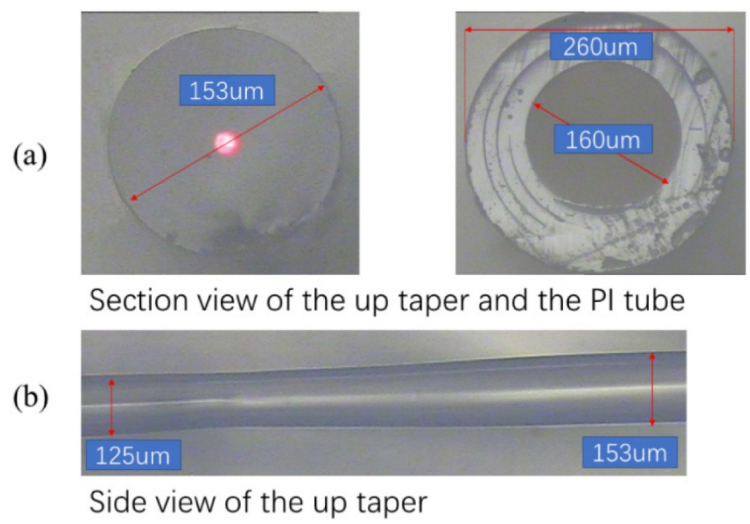

Fig. 2. Microscope image of the up-taper fiber and the PI tube

A two-beam optical interference equation can be used to describe the received intensity at the interrogator:

$$I_r = I_1 + I_2 + 2\sqrt{I_1 I_2}\cos(\frac{4\pi nl}{\lambda} + \varphi_0), \tag{1}$$

Optics EXPRESS

where I_r is the intensity of the interference signal; I_1 and I_2 are the intensity reflected from the cavity end faces, respectively; φ_0 is the initial phase of the interference; l is the cavity length; n is the refractive index of the air; λ is the optical wavelength in vacuum.

To demodulate the cavity length, there are several different methods. For a high-sensitivity application, the phase tracking method is used widely.

According to Eq. (1), when the phase of the cosine term satisfies:

$$\frac{4\pi nl}{\lambda}+\varphi_0=(2m+1)\pi\ (m=1,2,\ldots), \tag{2}$$

the interference signal emerges minimal value. The corresponding wavelength λ_m is the central wavelength of the mth order dip in the reflective spectrum.

$$\lambda_m=\frac{4\pi nl}{(2m+1)\pi\text{-}\varphi_0}. \tag{3}$$

Suppose the initial cavity length is l_0; the corresponding central wavelength of the mth order dip is λ_{m0} ; the axial strain on the tube is ε. The strain sensitivity of the sensor S_p is

$$S_p=\frac{\Delta\lambda_m}{\varepsilon}=\frac{4\pi n\Delta l}{(2m+1)\pi\text{-}\varphi_0}\cdot\frac{1}{\varepsilon}=\lambda_{m0}\cdot\frac{L}{l_0}. \tag{4}$$

Equation (4) shows that the sensitivity is determined by the ratio of the tube length to the cavity length. Assuming the length of the F-P cavity and the tube is 60 μm and 10 mm, the initial center wavelength of dip is 1500 nm, the sensitivity can be calculated by Eq. (4) as

$$S_p=1500\text{nm}\times\frac{10\text{mm}}{60\mu\text{m}}=0.25\text{nm}/\mu\varepsilon. \tag{5}$$

The strain sensitivity is >250 times compared with a typical FBG sensor (approximately 1 pm/ $\mu\varepsilon$). The phase tracking method has a high sensitivity; however, the dynamic range is narrow. For a light source with a spectrum width of 80 nm, the detectable strain change is approximately 320 με. For large strain measurement, the period tracking method is always used.

According to Eq. (1), the interference intensity I_r is not a cosine function of wavelength λ. However, according to Taylor' theorem, the Eq. (1) can be approximated as

$$\begin{aligned} I_r &\approx I_1+I_2+2\sqrt{I_1I_2}\cos\left(4\pi nl\left(\frac{1}{\lambda_0}\text{-}\frac{1}{\lambda_0^2}(\lambda\text{-}\lambda_0)\right)+\varphi_0\right)\\ &=I_1+I_2+2\sqrt{I_1I_2}\cos\left(\frac{4\pi nl}{\lambda_0^2}\lambda+\Phi_0\right). \end{aligned} \tag{6}$$

The intensity I_r is a cosine function of wavelength λ near the point $\lambda=\lambda_0$.

The period P of the cosine term satisfies:

$$P=\frac{2\pi}{\frac{4\pi nl}{\lambda_0^2}}=\frac{\lambda_0^2}{2nl}. \tag{7}$$

The cavity length l can be calculated by the period P which can be obtained from the Fourier transform of the reflected spectrum.

Optics EXPRESS

$$l = \frac{\lambda_0^2}{2nP} \tag{8}$$

Therefore, Eq. (8) can be used to calculate the absolute cavity length. Suppose the initial period is P_0, the axial strain ε is

$$\varepsilon = \frac{\Delta l}{l_0} = \frac{\lambda_0^2}{2n}\left(\frac{1}{P} - \frac{1}{P_0}\right) / l_0 = \frac{\lambda_0^2}{2nl_0P} - 1 = \frac{P_0}{P} - 1 . \tag{9}$$

If the temperature increases ΔT, the length of the PI tube also increases due to the thermal expansion. The change in temperature can be written as

$$\Delta T = \frac{1}{\alpha} \cdot \frac{\Delta l}{l_0} = \frac{1}{\alpha}\left(\frac{P_0}{P} - 1\right) \tag{10}$$

where the parameter α is the thermal expansion coefficient.

Equation (10) could be used to demodulate the temperature dependency.

3. Experimental results and discussion

To evaluate the performance of the proposed sensor for large-strain measurements, a sensor prototype is prepared. As shown in Fig. 3(a), the sensor is attached to a couple of three-degree-of-freedom precision stages. Hence, the strain can be precisely controlled. The initial length of the strain sensor is set to 10 mm. As the discussion in Eq. (9), the calibration strain is determined by dividing the change in the cavity length, directly measured by stage movement, by the initial length of the sensor. The strain detected by the sensor is calculated from an interference signal period.

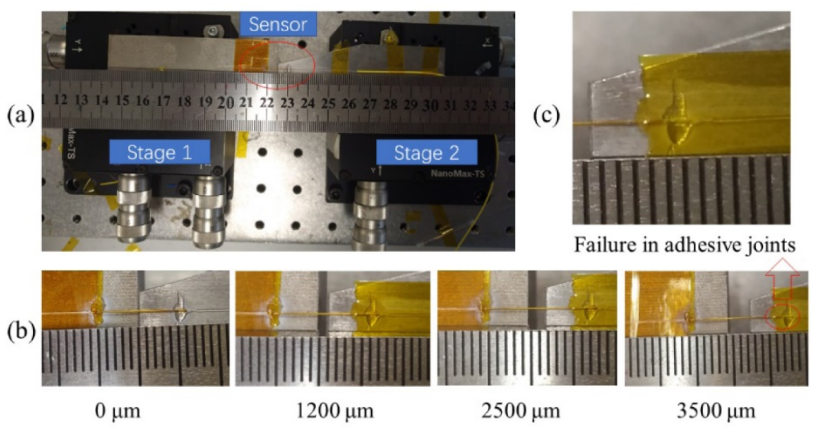

Fig. 3. (a) Experimental photos of the sensor fixed on the precision stages and (b) stretch process of the sensor

Figure 3(b) presents the stretching process of the sensor prototype from 0 μm and 3500 μm which corresponded a strain range is from 0 to 35%. It can be observed from the enlarged view of the glue in Fig. 3(c) that the PI tube begins to move with respect to the stage. The adhesive fails. The elongation of the sensor is longer than 3500 μm. The ultimate strain of the sensor is 35%.

Figure 4(a) shows four reflected spectrums of the F-P sensor prototype with different cavity lengths of 60 μm, 1260 μm, 2510 μm, and 3210 μm, respectively. They correspond to the strains of 0%, 12%, 25%, and 32%. The reflected spectrums are cosine function as discussed in Eq. (6). The period of the cosine function decreases as the F-P cavity length increases or as more fringes are condensed into a given observation spectrum range.

Optics EXPRESS

However, fringe visibility decreases as the F-P cavity length increases. The decrease of fringe visibility represents the signal-to-noise ratio deteriorates. The visibility influences the maximum cavity length which can be detected.

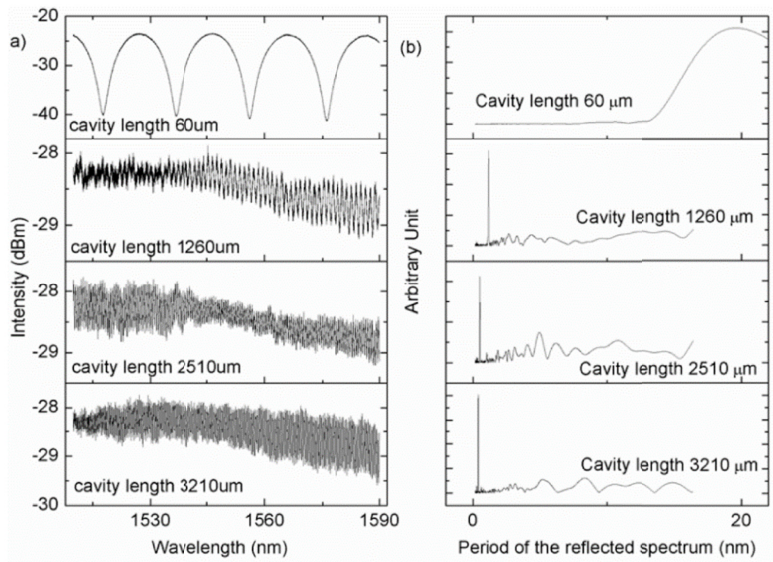

Fig. 4. (a) Reflected spectrum of the F-P cavity with different length and (b) FFT of the reflected spectrum

Figure 4(b) is the fast Fourier transform (FFT) results of the reflected spectrum. It can be observed clearly from the FFT result that each cavity length corresponds to one peak. The peak moves from right to left and its width becomes narrow as the cavity length increases. In Fig. 4(b), the major peak is much higher than others even if the cavity is stretched to 3210 μm. It implies that the signal-to-noise ratio can keep stable during the term of the stretch.

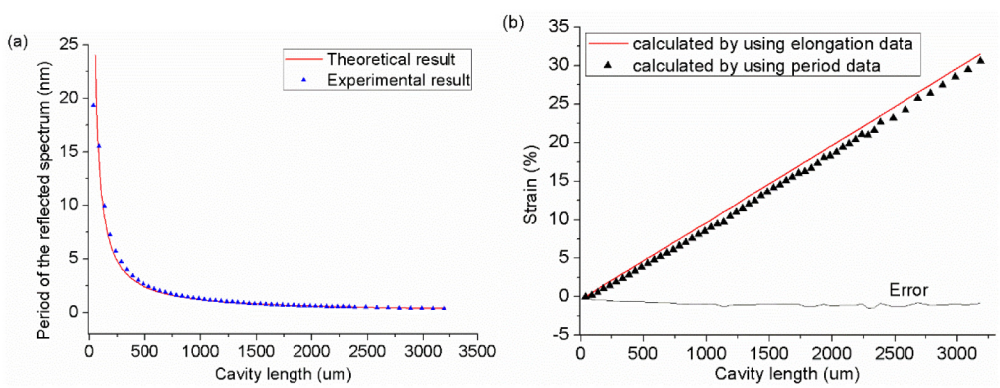

Fig. 5. (a) Period of the reflected spectrum of the F-P cavity and (b) strain in the PI tube with different cavity length

According to Eq. (7), the period of the reflected spectrum of the F-P cavity is inversely proportional to the cavity length. Figure 5(a) shows the inversely proportional relationship. The red line is the theoretical result calculated by Eq. (7) and the blue points are the experimental results. The experimental results are identical to the theoretical results. According to the inversely proportional relationship, a period of the reflected spectrum corresponds to an absolute cavity length. We can use the cavity length change to calculate the

Optics EXPRESS

axial strain in the PI tube. In the Eq. (9), the axial strain and the period of the reflected spectrum are also inversely proportional relationship. The strain sensitivity of the sensor can be described by

$$S = \frac{dP}{d\varepsilon} = -\frac{P_0}{(\varepsilon+1)^2}, \tag{11}$$

where P_0 is the initial period corresponding the initial cavity length l_0 and is equal to $\lambda_0^2 / 2nl_0$.

For small strain measurement, considering $\varepsilon < 2\%$, the strain sensitivity is approximately equal to - P_0 which corresponds the cavity length from 0 μm to 200 μm in Fig. 5(a). For large strain situation, the Eq. (11) shows the strain sensitivity increases rapidly which corresponds to the cavity length longer than 200 μm in Fig. 5(a).

Figure 5(b) shows the strain with different cavity length. Because of the highly stretchable hybrid silica/polymer structure, the proposed optical fiber sensor can endure much larger strain than the traditional silica fiber. The strain measurement range is between 0 and 35%. The red line is the calibration strain which is determined by dividing the change in the cavity length, directly measured by stage movement, by the initial length of the sensor. The black points represent the strains which are calculated by the period of the reflected spectrum. The difference between the results measured directly and those calculated by the period of the reflected spectrum is an error as shown in Fig. 5(b) with the black line. The error is less than 2% in a strain measurement range from 0 to 35%.

The period tracking method for calculating strain has a large dynamic range and a low sensitivity. However, the phase tracking method as described in Eq. (3) has opposite proprieties. It has a higher sensitivity and a smaller dynamic range. Combining two methods can resolve many special practical problems in applications. For example, some aerospace parts are made of the carbon fiber reinforced polymer (CFRP) which have to endure large-strain and high-temperature tests before they are assembled into a whole structure. The traditional optical fiber sensors embedded in CFRP material will be broken. After the assembly process is completed, the high sensitivity to the strain becomes a focus for monitoring the structural health of the aircraft. Therefore, both the large dynamic range and high sensitivity are important. The proposed hybrid silica/polymer optical fiber F-P sensor will be a candidate. The hybrid silica/polymer structure makes the sensor survive in the large strain test. The phase tracking method provides high sensitivity to the structural health monitoring process.

A sensor sample with a tube length of 5 mm is fabricated and fixed on the small strain calibration system as shown in Fig. 1(b). The reflected spectrum is shown in Fig. 6(a). The free spectrum range (FSR) is 6.02 nm which corresponds to a cavity length of 194 μm. The fringe will shift to the right as the strain increases. The sensitivity to the strain is shown in Fig. 6(b). In small strain calibration experiments, the sensor shows an excellent linear sensitivity. The experimental value is 28 pm/με which is lower than the theoretical value (38.75 pm). The difference may be caused by the glue at both ends of the PI tube that permeates into the tube. The stretchable part of PI tube shortens, then the sensitivity decreases. A step strain is loaded on the sample. In the experiment, the strain decreases by 15 με each time and repeated five times. And then the strain increases by 15 με each time until it recoveries. The response of the sensor is shown in Fig. 6(c). The sensor could distinguish the different strains rapidly. Fig. 6(d) shows the repeatability of the sensor. Eight loading/unloading cycles are implemented. The strain is alternately varied between 0 and 160 με. The sensor shows a slight zero-point drift. After each cycle, the zero points will raise by 2 με. It may be caused by the sluggishness of the PI tube.

Optics EXPRESS

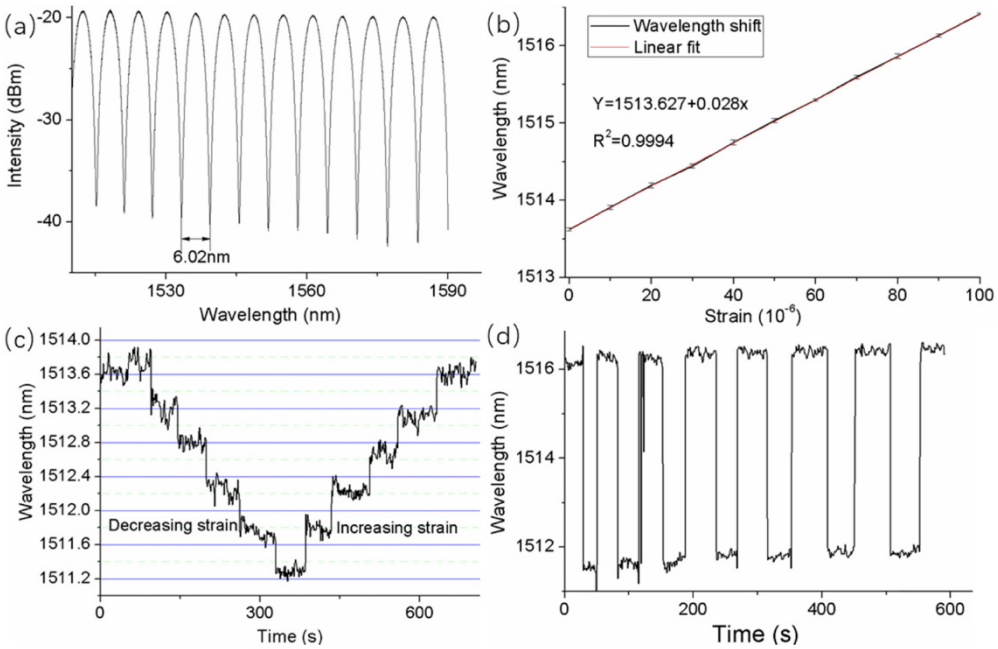

Fig. 6. (a) Reflected spectrum of the sensor; (b) relationship between the wavelength and the strain; (c) response of the sensor to the dynamic strain; (d) repeatability of the sensor in eight loading/unloading cycles

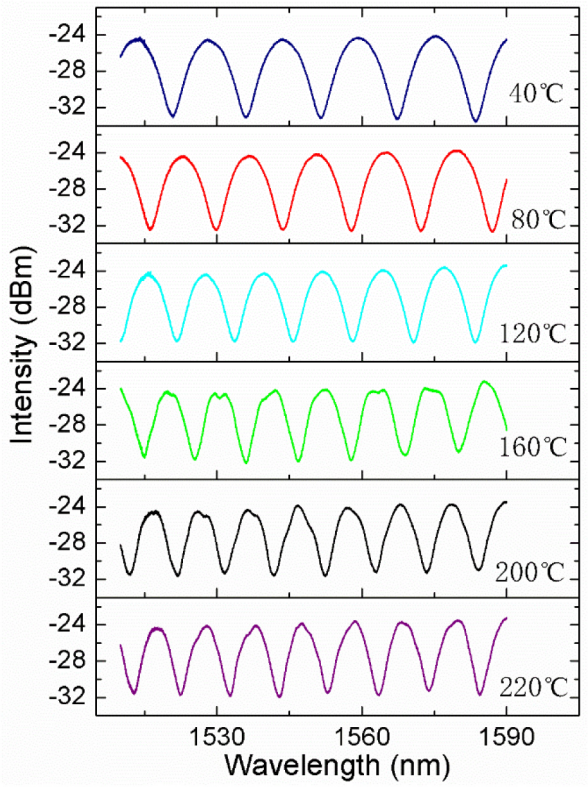

Fig. 7. Reflected spectrum of the F-P cavity with different temperature

Optics EXPRESS

To test the high-temperature sensitivity of the sensor, a sample with an 8mm PI tube is prepared. The schematic diagram of the test system is shown in Fig. 2(b). The calibration system is an oven whose temperature can be controlled by a computer. To obtain a stable reading at a certain temperature, the temperature in the oven is kept constant for one hour. After the temperature becomes stable, the reflected spectra of the sensor at different temperatures are recorded and shown in Fig. 7. The period of the fringe shortens as the temperature increases from 40 °C to 220 °C. Thanks to the excellent high-temperature endurance of PI and adhesive, the sensor does not fail in 220 °C ambiance. Because of the high-temperature load, the phase tracking method is invalid. The period tracking method was used to evaluate the temperature. Figure 8(a) shows the FFT results of the reflected spectrum. In high-temperature ambiance, the reflected spectrums of sensor keep single-frequency oscillation. Each FFT result is a single-peak function. The peak shifts to the left as the temperature increases. Figure 8(b) shows that the sensitivity to the temperature gradually decreases as the temperature increases. Above 200 °C, the change of the reflected spectrum is insensitive to the temperature.

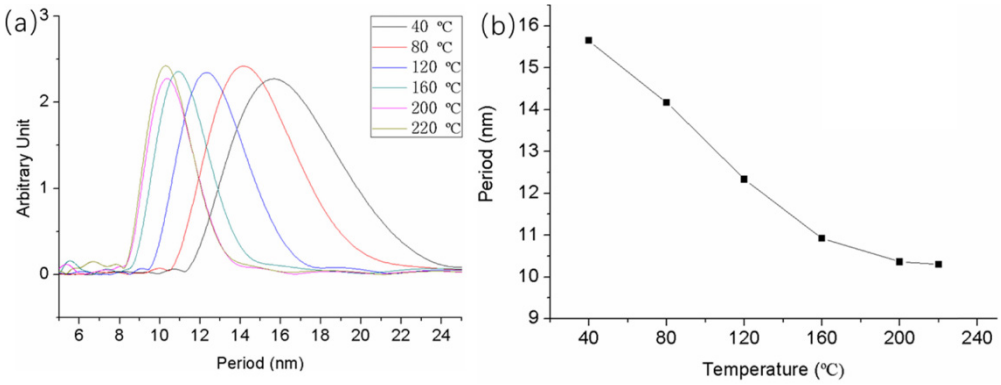

Fig. 8. (a) FFT of the reflected spectrum in Fig. (7); (b) Calibration curve between the temperature and the period.

4. Conclusion

To implement large-strain and high-sensitivity measurement in high-temperature ambiance, a hybrid silica/polymer optical fiber F-P sensor is proposed. The sensor consists of a section of continuous PI tube and two fibers. The ends of fibers form an F-P cavity in the PI tube. The end faces of silica optical fiber can move freely as the PI tube stretches. Therefore, the hybrid structure can endure the extraordinarily large strain, and keep the high sensitivity to the strain. Because of the excellent high-temperature endurance of PI and adhesive, the sensor can work in high-temperature ambiance. According to the different requirements in the large-strain measurement and high-sensitivity measurement, the period tracking method and the phase tracking method are introduced. The sensitivity and dynamic range of the hybrid structure sensor are analyzed theoretically. The simulation results show the sensor has a large dynamic range and high sensitivity. To verify the design, several samples are prepared and tested. The experimental results show the structure can endure an ultimate tensile strain of 35%. It is 35 times larger than that of traditional fiber. When a phase tracking method is used, the sensor has a high strain sensitivity (28 pm/με) which is 28 times larger than that of the traditional FBG sensors. In addition, the sensor can resist the high temperature of up to 220 °C. The large-strain, high-sensitivity, and high-temperature performances indicate that the proposed hybrid silica/polymer optical fiber F-P sensor has potentials in extreme measurements including monitoring deformation in plastic products, monitoring health in CFRP space parts, and even monitoring strain in biomaterials.

Optics EXPRESS

Funding

OCPC International Postdoctoral Program of China, GRF 152113317, Hong Kong Polytechnic University, 1-ZVGB.

References

1. Y. W. Huang, J. Tao, and X. G. Huang, "Research Progress on F-P Interference-Based Fiber-Optic Sensors," Sensors (Basel) **16**(9), 1424 (2016).
2. Y. Liu and J. Zhang, "Model Study of the Influence of Ambient Temperature and Installation Types on Surface Temperature Measurement by Using a Fiber Bragg Grating Sensor," Sensors (Basel) **16**(7), 975 (2016).
3. Y. Liu, Y. Li, P. Huang, H. Song, and G. Zhang, "Modeling of hydrogen atom diffusion and response behavior of hydrogen sensors in Pd-Y alloy nanofilm," Sci. Rep. **6**(1), 37043 (2016).
4. M. Yucel and N. F. Ozturk, "Real-time monitoring of railroad track tension using a fiber Bragg grating-based strain sensor," Instrum. Sci. Technol. **46**(5), 519–533 (2018).
5. X. W. Ye, Y. H. Su, and P. S. Xi, "Statistical Analysis of Stress Signals from Bridge Monitoring by FBG System," Sensors (Basel) **18**(2), 491 (2018).
6. M. J. Nicolas, R. W. Sullivan, and W. L. Richards, "Large Scale Applications Using FBG Sensors: Determination of In-Flight Loads and Shape of a Composite Aircraft Wing," Aerospace **3**(3), 18 (2016).
7. M. Liu, E. Zhang, Z. Zhou, Y. Tan, and Y. Liu, "Measurement of Temperature Field for the Spindle of Machine Tool Based on Optical Fiber Bragg Grating Sensors," Adv. Mech. Eng. **5**, 940626 (2013).
8. Y. Huang, Z. Zhou, Y. Zhang, G. Chen, and H. Xiao, "A Temperature Self-Compensated LPFG Sensor for Large Strain Measurements at High Temperature," IEEE Trans. Instrum. Meas. **59**(11), 2997–3004 (2010).
9. L. Zhang, X. Chang, Y. Zhang, and F. Yang, "Large Strain Detection of SRM Composite Shell Based on Fiber Bragg Grating Sensor," Photonic Sens. **7**(4), 350–356 (2017).
10. H. Y. Liu, H. B. Liu, and G. D. Peng, "Tensile strain characterization of polymer optical fibre Bragg gratings," Opt. Commun. **251**(1-3), 37–43 (2005).
11. J. Huang, X. Lan, H. Wang, L. Yuan, T. Wei, Z. Gao, and H. Xiao, "Polymer optical fiber for large strain measurement based on multimode interference," Opt. Lett. **37**(20), 4308–4310 (2012).
12. Y. Huang, T. Wei, Z. Zhou, Y. Zhang, G. Chen, and H. Xiao, "An extrinsic Fabry–Perot interferometer-based large strain sensor with high resolution," Meas. Sci. Technol. **21**(10), 105308 (2010).
13. H. Huang, A. Majumdar, and J. Cho, "Fabrication and evaluation of hybrid silica/polymer optical fiber sensors for large strain measurement," T. I. Meas. Control **31**(3-4), 247–257 (2009).